World Journal of Gastroenterology

Online Submissions: http://www.wjgnet.com/1007-9327office
wjg@wjgnet.com
doi:10.3748/wjg.v17.i31.3614

World J Gastroenterol 2011 August 21; 17(31): 3614-3622
ISSN 1007-9327 (print) ISSN 2219-2840 (online)

ORIGINAL ARTICLE

Bimodal visualization of colorectal uptake of nanoparticles in dimethylhydrazine-treated mice

Tao Wu, Wei-Liang Zheng, Shi-Zheng Zhang, Ji-Hong Sun, Hong Yuan

Tao Wu, Wei-Liang Zheng, Shi-Zheng Zhang, Department of Radiology, Sir Run Run Shaw Hospital, School of Medicine, Zhejiang University, No. 3 Qingchun Road East, Hangzhou 310016, Zhejiang Province, China
Tao Wu, Department of Radiology, Jining Medical College, Jining 272067, Shandong Province, China
Ji-Hong Sun, Department of Radiology, Second Affiliated Hospital, Zhejiang University School of Medicine, Hangzhou 310009, Zhejiang Province, China
Hong Yuan, College of Pharmaceutical Sciences, Zhejiang University, Hangzhou 310009, Zhejiang Province, China
Author contributions: Wu T, Zheng WL, and Zhang SZ designed the research; Wu T, Zheng WL and Sun JH performed the research; Yuan H designed and evaluated the nanoparticles; Wu T analyzed the data and wrote the paper; Zhang SZ guaranteed the integrity of the research.
Supported by National Natural Science Foundation of China, No. 30670610.
Correspondence to: Shi-Zheng Zhang, MD, Professor of Radiology, Department of Radiology, Sir Run Run Shaw Hospital, School of Medicine, Zhejiang University, No. 3 Qingchun Road East, Hangzhou 310016, Zhejiang Province, China. paper.wutao@gmail.com
Telephone: +86-571-86006751 Fax: +86-571-86032876
Received: December 4, 2010 Revised: March 24, 2011
Accepted: April 3, 2011
Published online: August 21, 2011

Abstract

AIM: To investigate colorectal uptake of solid lipid nanoparticles (SLNs) in mice receiving different doses of 1,2-dimethylhydrazine (DMH) using magnetic resonance (MR) and laser-scanning confocal fluorescence microscope (LSCFM) imaging.

METHODS: Eight mice were sacrificed in a pilot study to establish the experimental protocol and to visualize colorectal uptake of SLNs in normal mice. Gadopentetate dimeglumine and fluorescein isothiocyanate (FITC)-loaded SLN (Gd-FITC-SLN) enemas were performed on mice receiving DMH for 10 wk (group 1, n = 9) or 16 wk (group 2, n = 7) and FITC-SLN enema was performed on 4 DMH-treated mice (group 3). Pre- and post-enema MR examinations were made to visualize the air-inflated distal colorectum. Histological and LSCFM examinations were performed to verify colorectal malignancy and to track the distribution of SLNs.

RESULTS: Homogeneous enhancement and dense fluorescence (FITC) deposition in colorectal wall were observed in normal mice and 1 DMH-treated mouse (group 1) on fluid attenuated inversion recovery (FLAIR) and LSCFM images, respectively. Heterogeneous mural enhancement was found in 6 mice (4 in group 1; 2 in group 2). No visible mural enhancement was observed in the other mice. LSCFM imaging revealed linear fluorescence deposition along the colorectal mucosa in all groups. Nine intraluminal masses and one prolapsed mass were detected by MR imaging with different enhancement modes and pathologies. Interstitial FITC deposition was identified where obvious enhancement was observed in FLAIR images. Bladder imaging agent accumulations were observed in 11 of 16 DMH-treated mice of groups 1 and 2.

CONCLUSION: There are significant differences in colorectal uptake and distribution of SLNs between normal and DMH-treated mice, which may provide a new mechanism of contrast for MR colonography.

Key words: Solid lipid nanoparticles; Colorectal cancer; Magnetic resonance colonography

Peer reviewer: Reiji Sugita, MD, Departments of Radiology, Sendai City Medical Center, 5-22-1, Tsurugaya, Miyagino-ku, Sendai 983-0824, Japan

Wu T, Zheng WL, Zhang SZ, Sun JH, Yuan H. Bimodal visualization of colorectal uptake of nanoparticles in dimethylhydrazine-treated mice. *World J Gastroenterol* 2011; 17(31): 3614-3622 Available from: URL: http://www.wjgnet.com/1007-9327/full/v17/i31/3614.htm DOI: http://dx.doi.org/10.3748/wjg.v17.i31.3614

INTRODUCTION

Colorectal imaging examinations consist of double-contrast barium enema (DCBE), colonoscopy, computed tomography (CT) colonography and magnetic resonance (MR) colonography. The four methods have their advantages and disadvantages. Colonoscopy, however, is the dominant technique for colorectal examination due to its high diagnostic sensitivity and capability for immediate intervention and histological evaluation. Despite the merits and continuous technical innovation, colonoscopy, as an invasive test, is not well accepted in a screening setting and cannot be performed on certain conditions such as inflammatory or malignant bowel stenosis. MR colonography, introduced in the last decade, has demonstrated encouraging initial results in the detection of polyps greater than 1 cm in diameter. Unlike CT colonography, MR colonography is a "pure noninvasive" test because it is ion-free[1-3].

High contrast between the bowel wall and lumen, implemented by either "dark-lumen" or "bright-lumen" technique, is essential for successful MR colonography. The contrast mechanisms depend on the combination of ultrafast MR sequences and an appropriate rectal enema recipe[3-7]. In most cases, a low uptake of bowel contrast agents means low toxicity. To the best of our knowledge, no radiological research aiming at visualizing the uptake of bowel contrast agents has been described.

Recently, however, intestinal uptake of particulate matter in the micro- and nanometer range has been a hot topic in pharmacological research. Studies on oral delivery of insulin, vaccine and a set of hydrophobic drugs using various nano-vehicles are under way[8-13]. Solid lipid nanoparticles (SLN) are colloidal carriers for controlled drug delivery introduced after the development of emulsions, liposomes, polymer-based microparticles and nanoparticles. SLN combines the advantages of polymeric nanoparticles and oil/water fat emulsions for drug delivery, such as good tolerability, high oral bioavailability and feasibility, for large-scale production[14] .

The aim of this study is to exemplify the feasibility of using colorectal uptake of SLNs as an extra source of contrast in colonography. To model non-familial colorectal carcinoma (CRC) in rodents, 1,2-dimethylhydrazine (DMH), a specific colon carcinogen, was administered to the mice to produce CRC and impair the bowel wall. Colorectal uptake of SLNs in mice receiving different doses of DMH was investigated using MR and laser-scanning confocal fluorescence microscope (LSCFM) imaging.

MATERIALS AND METHODS

Synthesis of SLNs

Fluorescein isothiocyanate-labeled octadecylamine (ODA-FITC) and gadopentetate dimeglumine (Gd-DTPA) loaded SLNs (Gd-FITC-SLN) were synthesized by "solvent diffusion method in a nano-reactor system," as described previously [15]. Briefly, Gd-DTPA (25 mg) and Tween 80 (18 mg) were dissolved in water (1 mL) to prepare the "aqueous phase". The water in an oil mini-emulsion was obtained by mixing, stirring and ultrasonic treatment of the "aqueous phase" and the "oil phase," which consisted of Span 80 (200 mg) and n-Hexane (10 mL). A mixture of 45 mg monostearin and 5 mg ODA-FITC, dissolved in 1 mL ethanol in a 60 ℃ water bath, was quickly dispersed into the mini-emulsion under mechanical agitating at 400 for 5 min. The dispersion was centrifuged for 15 min at 20 000 r/min to precipitate SLNs, which were subsequently washed twice with n-hexane and re-dispersed in Poloxamer 188. The resultant SLNs, dispersed to equal milligrams of manicol, were freeze-dried and kept away from light at 4 ℃. Both Gd-DTPA and ODA-FITC were omitted to produce blank SLN; only one of the imaging agents, Gd-DTPA or ODA-FITC, was added to synthesize Gd-SLN or FITC-SLN. The physicochemical properties of the SLNs were characterized as documented previously [11,15].

Pilot study

All animal experiments were approved by the institutional animal care and use committee and performed in accordance with the committee's regulations. The mice were deprived of food and allowed to drink 5% glucose saline 24 h before the examination to clean the gastrointestinal tract. An intra-peritoneal injection of pentobarbital (50 mg/kg body weight) was performed before any surgical manipulation. Eight male Kunming mice (22-25 g) were sacrificed in the pilot study. An operative procedure was established to limit enema within the distal colorectum.

MR pulse sequence (SE T2WI and FLAIR) and microscopic fluorescence imaging techniques were evaluated. The concentration of enema agents, including Gd-DTPA solution, Gd-SLN, FITC-SLN and Gd-FITC-SLN suspensions, were adjusted according to MR and fluorescence image findings. Qualified data from the pilot study were included into the study results.

Animal model and groups

Subcutaneous injection of DMH (20 mg/kg body weight) was performed wkly on 5-wk-old Kunming mice for 10 (n = 15) and 16 wk (n = 15) to induce colorectal tumors. Ten mice were excluded from the study due to DMH- and anesthesia-related mortality (n = 7) and operation failures (n = 3).

Gd-FITC-SLN (40 mg/mL) enema was performed on 9 mice receiving DMH for 10 wk (group 1) and 7 mice receiving DMH for 16 wk (group 2). FITC-SLN (40 mg/mL) enemas were performed on 4 mice (group 3) receiving DMH for 10 (n = 2) and 16 wk (n = 2).

Operative procedure

After anesthesia, an abdominal incision was made into the peritoneal cavity, and the sigmoid colon was ligated. The peritoneal cavity was then closed by two layers of continuous sutures. Subsequently, the distal colorectum was slightly inflated by infusing about 0.3 mL room air *via* the anal orifice and gently ligating tissues around to prevent air leakage. Thus, the mouse was ready for the

pre-enema MR examination. After the pre-enema MR test, an SLN enema was performed for 20 min by infusing 0.3-0.4 mL of the dispersion into the rectal lumen and ligating tissues around the anus. In-enema MR imaging was performed during the enema process. After the enema was performed and the anal ligate was removed, the enema agents were cleared by warm saline coloclysis. The distal colorectal lumen was then inflated by air again for the post-enema MR examinations, performed 25 and 60 min after the SLN enema was started. The mice were warmed by placing a hot water bag aside during the experiment.

MR imaging and analysis

Image acquisition was performed with a 1.5 T clinical MR device (Signa 1.5 T; GE Medical Systems, Milwaukee, Wis). A 5-cm custom-built coil was used for signal emission and reception. Animals were examined in the supine position. Transverse FLAIR MR images from sigmoid colon to the anus were acquired using the following parameters: repetition time, 2000 ms; echo time, 11.1 ms; inversion time, 750 ms; section thickness, 2 mm; intersection gap, 0 mm; field of view, 6-8 cm; matrix, 320 × 192; number of signals acquired, one. Transverse T2WI imaging (repetition time, 3860 ms; echo time, 106.0 ms) with the same section thickness and image size was also performed. Multi-planar FLAIR and T2WI imaging were performed continuously if colorectal masses had been detected in initial imaging.

The MR images of the colorectal wall and masses were at first interpreted in consensus by two radiologists with 20 and 10 years of experience, respectively. Colorectal masses were located by measuring the mass to anus distance. Then, quantitative analysis was performed based on the recommended procedure[16]. First, identical axial FLAIR slices before and after enema were selected for region of interest (ROI) definition. Second, a curved ROI encompassing the colorectal wall or an irregular ROI encompassing the intraluminal mass, a round ROI on the back or pelvic muscle and an oval ROI along the phase encoding direction encircling air were defined; the signal intensity (SI) values were recorded (Image J, version 1.38; National Institutes of Health, Bethesda, MD). Third, Third, the the SI difference–to-noise ratios (SDNRs) for the colorectal wall or tumors were calculated using the following formula: SDNR = (SIt-SIm)/SDN, where SIt is the mean SI value of target (the colorectal wall or intraluminal mass); SIm, the mean SI of the muscle; and SDN, the standard deviation of the background noise (air).

Histopathologic and fluorescent evaluation

Animals were euthanized by an overdose of pentobarbital immediately after MR examination. The colorectum was harvested. The macroscopic morphology of the bowel as well as the location and size of the masses within the ligated distal colorectum were recorded. The colorectal wall and masses were then sampled, frozen with liquid nitrogen, and cut into 5-7 μm slices with a microtome for LSCFM (Leica TCS-SP5, Wetzlar, Germany) evaluation and HE slice preparation. Diamidinophenyl-indole (DAPI 1:15 000 dilution, Sigma, St. Louis, MO, United States) staining was performed on slices of one normal mouse to visualize the nuclei of intestinal cells. FITC carried by SLNs was excited at 488 nm and detected at 500-535 nm wavelengths. DAPI was excited at 405 nm and detected at 430-550 nm. The remaining tissues were sampled and immerged in 10% buffered formalin to prepare the standard hematoxylin and eosin (HE)-stained slices.

Statistical analysis

SDNR data of colorectal wall, intraluminal mass size and other observations were expressed as means ± standard deviations. Statistical analysis was performed with software (SPSS for Windows, release 16.0; SPSS, Chicago). One-way analysis of variance with least significant difference tests was applied for multiple comparisons of pre- and post-enema SDNRs of the colorectal wall (groups 1-3) and SDNRs of intraluminal masses (groups 2 and 3). P value < 0.01 was considered a significant difference.

RESULTS

Characterization of SLNs

SLNs exhibited bimodal particle sizes ranging from 50 to 300 nm and zeta potentials ranging from - 29.3 ± 3.4 to - 39.1 ± 2.0 mV. The particle size increased slightly as ODA-FITC was loaded. Entrapment efficiency for Gd-DTPA in Gd-SLNs or in Gd-FITC-SLNs was 55.8% or 55.0%, respectively. Loading capacity of Gd-DTPA in Gd-SLNs or Gd-FITC-SLNs was about 50%. Hence, 40 mg Gd-FITC-SLN or Gd-SLN freeze-dried powder dispersed in 1 mL water, as used in the current study, contains about 10 mg Gd-DTPA and 20 mg Mannitol. MR images of SLN dispersions and pure water are shown in Figure 1.

Pilot study findings

Four mice were sacrificed to establish the experimental protocol. The colorectal wall was detectable on FLAIR (low-SI) and T2WI (iso- to high-SI) images. However, bowel layers could not be differentiated. While LSCFM (Leica TCS-SP5, Germany) provided fine fluorescent images, the fluorescence microscope (Zeiss Axioskop 2, Carl Zeiss, Marburg, Germany) seemed applicable in tracking the distribution of FITC-loaded SLNs.

Homogeneous mural enhancement on post-enema FLAIR images was observed after Gd-SLN (n = 1) and Gd-FITC-SLN (n = 2, 20/22 slices) retention enema. Dense FITC deposition was observed in fluorescence imaging after FITC-SLN (n = 1) and Gd-FITC-SLN enema (Figure 2). No positive MR or fluorescence image finding was observed after Gd-DTPA solution (n = 1) enema.

MR and LSCFM image features of colorectal wall and pathologic correlation

MR data of only 20 of the 30 DMH-treated mice were

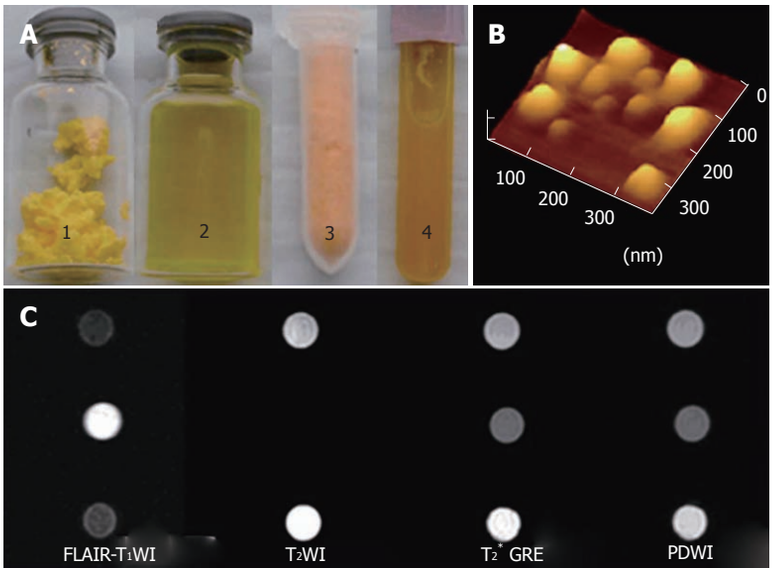

Figure 1 Characterization of solid lipid nanoparticles. A: Gadopentetate dimeglumine and fluorescein isothiocyanate-loaded solid lipid nanoparticles (Gd-FITC-SLNs) freeze-dried powder (1) and dispersion (2); Fluorescein isothiocyanate solid lipid nanoparticles (FITC-SLNs) freeze-dried powder (3) and dispersion (4); B: Atomic force microscopy images of blank solid lipid nanoparticles; C: Magnetic resonance (MR) images of FITC-SLNs dispersions (top). Gd-FITC-SLN suspension (middle). Water (bottom) obtained with fluid attenuated inversion recovery (FLAIR) (left), T_2WI (middle left), T_2* GRE (middle right) and PDWI (right). FLAIR was obtained with the following parameters: 2000/11.1/750/2, TR/TE/TI/NEX; T2WI: 3860/106/2 (TR/TE/NEX); T_2* GRE: 550/14/2/200 (TR/TE/NEX/Flip); PDWI: 3220/12/1 (TR/TE/NEX). Both sequences used a 256 × 160 matrix, a 140 mm FOV, and 4-mm-thick sections.

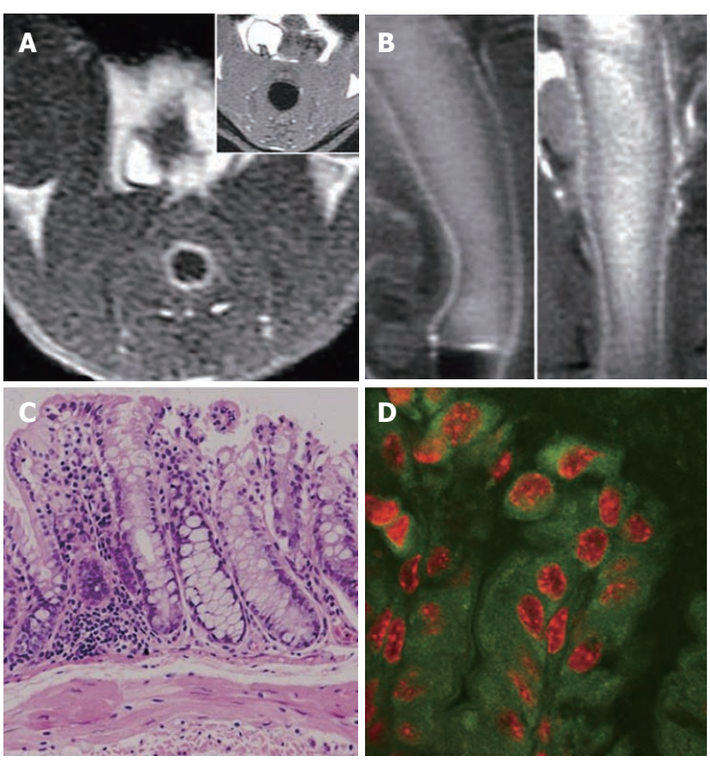

Figure 2 Magnetic resonance and fluorescent images of colorectal wall in normal mouse and bright rim sign in 1,2-dimethylhydrazine treated mouse. A: Axial fluid attenuated inversion recovery (FLAIR) image 5 min after gadopentetate dimeglumine and fluorescein isothiocyanate (FITC)-loaded solid lipid nanoparticle enema, showing the homogeneous mural enhancement; B, C: No abnormity was found in hematoxylin and eosin slices of the mouse; D: Laser-scanning confocal fluorescence microscope image of the post-enema colorectal wall of normal mouse with diamidino-phenyl-indole (DAPI) stain, showing the dense cytoplastic FITC deposition and red DAPI-stained nucleus.

available due to DMH- and anesthesia-related mortality (n = 7) and operation failures (n = 3). In group 1, homogeneous enhancement and dense FITC deposition were observed in 1 mouse (8/10 slices) with no histological abnormity; the enhanced colorectal wall manifested as a bright rim sign on in-enema FLAIR images (Figure 2B). Heterogeneous enhancement was observed in 4 of the other 8 mice (26/48 slices). No visible mural enhancement was identified in the other 4 mice; mild dysplasia was identified in HE slices of the 8 mice with linear FITC deposition observed along the intestinal lumen in LSCFM images (Figure 3). In group 2, heterogeneous enhancement was shown in 2 of the 7 mice (6/16 slices); no other mural enhancement was observed. In group 3, no enhancement was found on FLAIR images after the FITC-SLN enema. Obvious dysplasia and intraepithelial neoplasia (low to high grade) were found in HE slices of mice receiving DMH for 16 wk (groups 2 and 3) with linear FITC deposition along the intestinal lumen observed in LSCFM images. Non-enhanced colorectal walls manifested as low signal rings around the "bright lumen" in in-enema FLAIR images, which was observed in 4 of the 7 mice in group 2 (Figure 4B).

MR and LSCFM findings of colorectal mass in DMH groups and pathologic correlation

MR detected 9 intraluminal masses (short axis 2.06 ± 0.98 mm) and 1 prolapsed mass (well-differentiated squamous

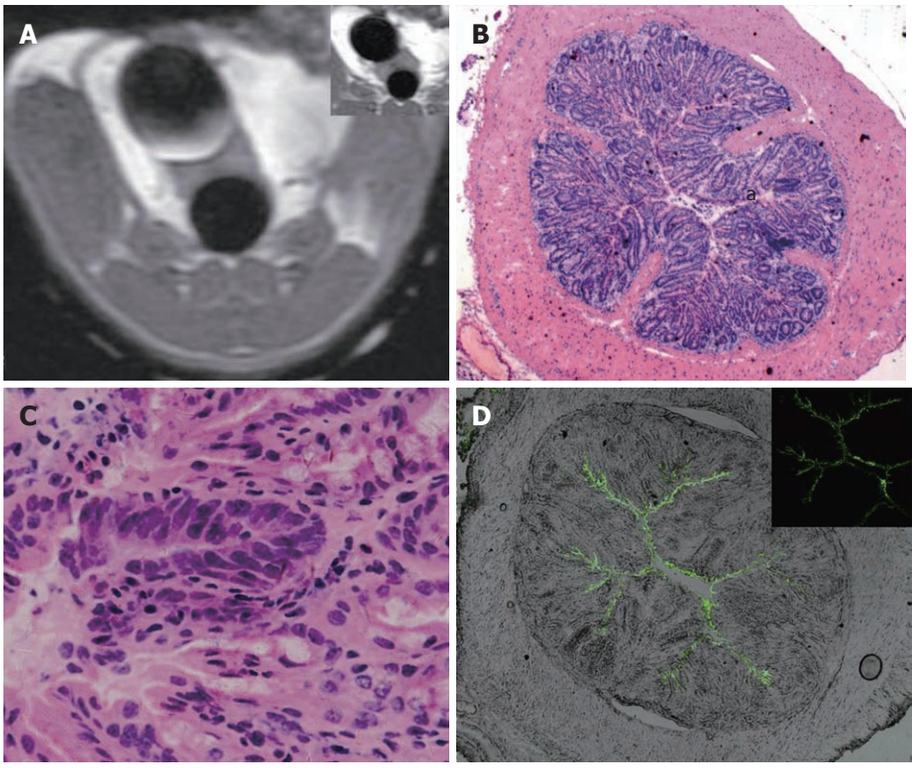

Figure 3 Magnetic resonance and fluorescent images of 1,2-dimethylhydrazine impaired colorectal wall. A: Axial fluid attenuated inversion recovery (FLAIR) image 5 min after gadopentetate dimeglumine (Gd-DTPA) and fluorescein isothiocyanate (FITC)-loaded solid lipid nanoparticle enema. No mural enhancement was identified. Note the bladder Gd-DTPA deposition (top right: pre-enema FLAIR image); B, C: Hematoxylin and eosin image of the same slice; nuclear atypia identified; B: × 40; C: × 400. D: Laser-scanning confocal fluorescence microscope image of the post-enema colorectal wall, showing the linear extracellular FITC deposition along the mucosa.

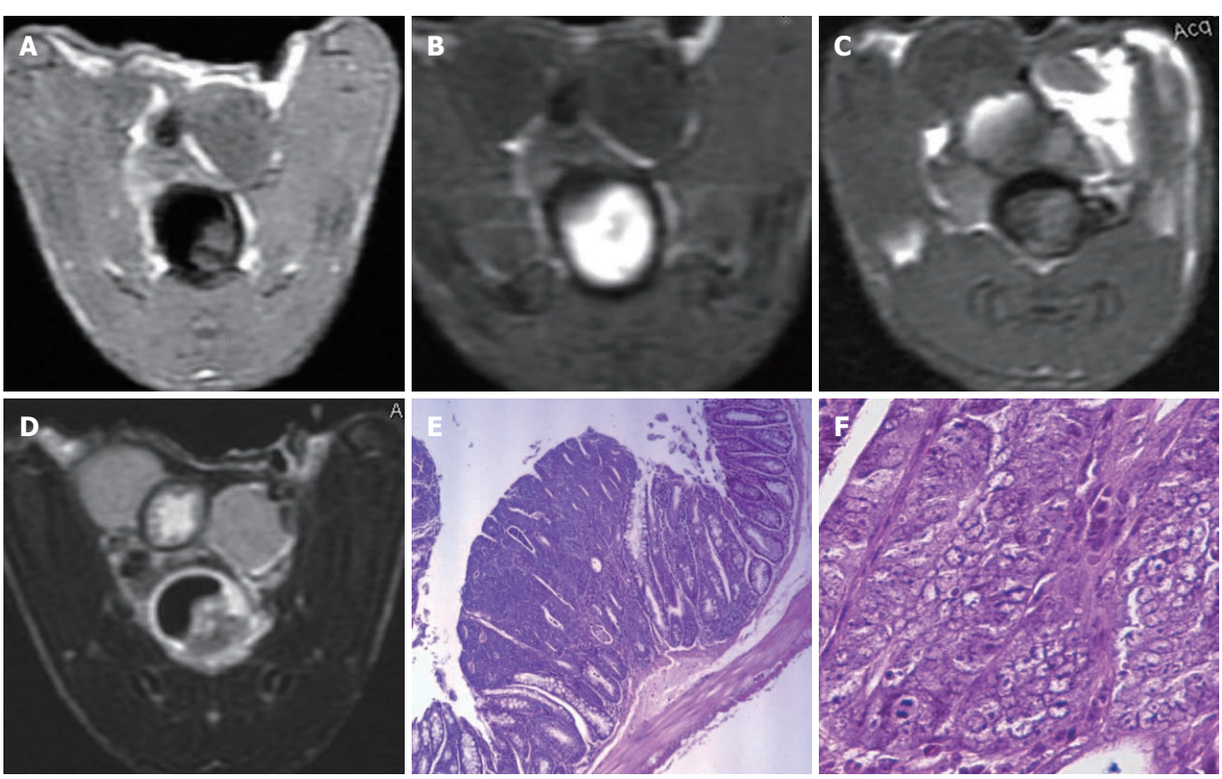

Figure 4 Magnetic resonance and histological images of adenocarcinoma. A: An irregular-shaped mass in the pre-enema fluid attenuated inversion recovery (FLAIR) image; B: Low signal ring around the bright lumen (halo sing) in the in-enema FLAIR image; C: Tumor enhancement and bladder imaging agents accumulation both occurred in the post-enema FLAIR image; D: T2 weighted post-enema image, heterogeneous signal intensity within the tumor; E, F: Hematoxylin and eosin images of the tumor, adenocarcinoma cells identified.

carcinoma) in groups 2 and 3. Eight of the 9 intraluminal masses were adenomas with different levels of malignancy; one of them was histologically proven as adenocarcinoma. The intraluminal masses manifested as filling deficits on Gd-FITC-SLN inflated bright-lumen FLAIR images. No visible enhancement was found in post-enema

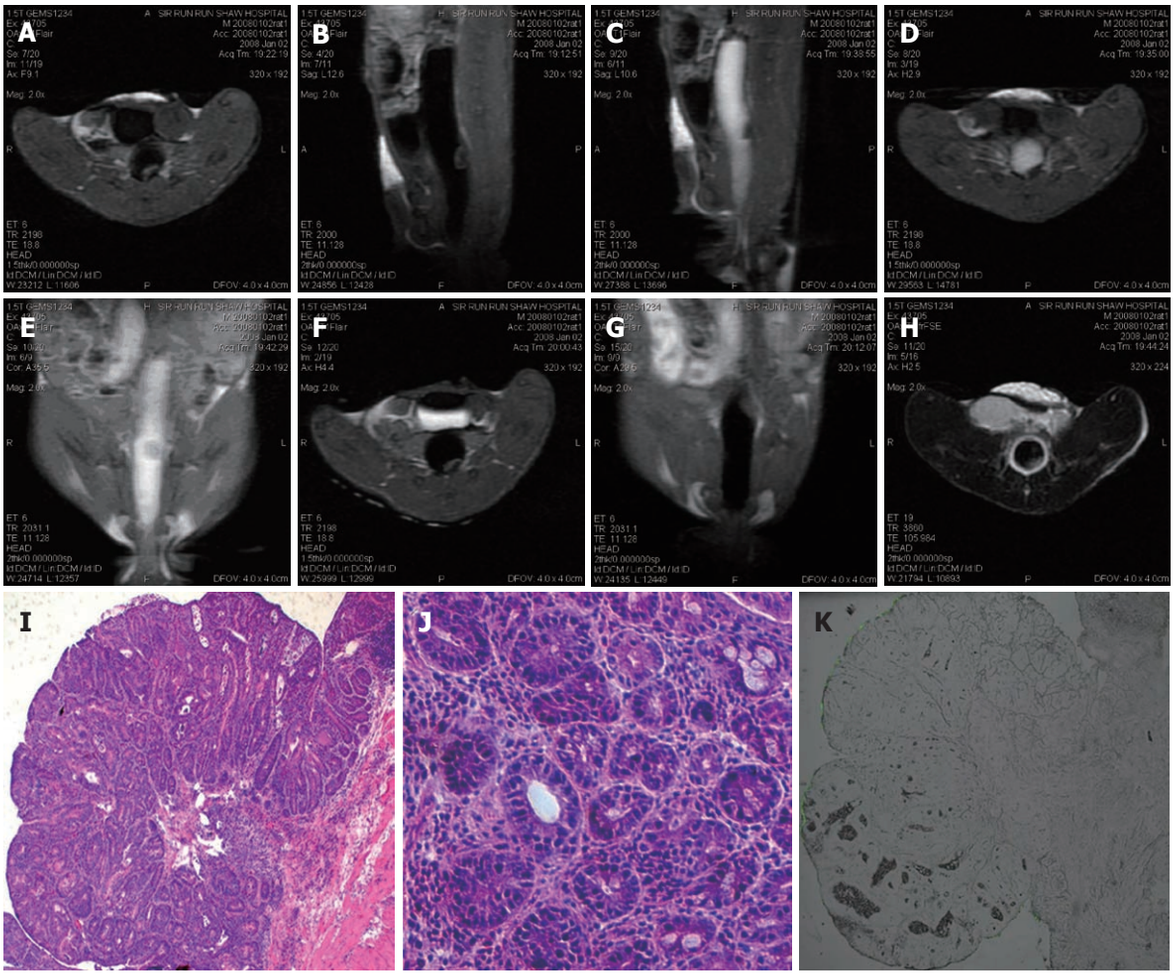

Figure 5 Magnetic resonance and fluorescent images of a non-enhanced adenoma. A, B: Axial and sagittal pre-enema fluid attenuated inversion recovery (FLAIR) images, note the inner low signal of the mass; C-E: The mass manifests as a filling deficit in the gadopentetate dimeglumine (Gd-DTPA) and fluorescein isothiocyanate-loaded solid lipid nanoparticle (Gd-FITC-SLN) enema inflated FLAIR images; F, G: No enhancement identified after the enema. Note the bladder Gd-DTPA deposition; H: Axial T2 weighted image after the Gd-FITC-SLN enema. Iso-signal observed in the adenoma; high signal observed for the bowel wall; I-K: Hematoxylin and eosin and laser-scanning confocal fluorescence microscope images of the adenoma.

FLAIR images in one narrow-based adenoma with minimum FITC deposition along the edge and within the mass (Figure 5). Various degrees of enhancement were found in the other masses with interstitial FITC depositions in LSCFM images (Figure 6).

Other MR and pathohistologic findings

Colorectum stiffness was observed in 3 of 9 mice (groups 2 and 3) receiving DMH for 16 wk. Macroscopic evaluation of the animal's distal colorectum revealed an extra adenoma measuring 2 × 3 mm in size in the sigmoid colon, which was missed in MR examination. No false-positive MR findings were observed by postmortem evaluation. Bladder imaging agent accumulation was accidently found in 11 of the 16 DMH-treated mice (groups 1 and 2) 3 - 28 (11.2 ± 9.6) min after the Gd-FITC-SLN enema was started (Figures 3-6).

Statistical results

Pre- and post-enema SDNR values of colorectal wall in each group and intraluminal masses in DMH-treated mice were plotted against time (Figure 7) with brief annotation.

DISCUSSION

We used MR and LSCFM to study the colorectal uptake of SLNs. The bimodal imaging used elsewhere for tumor angiogenesis and lymphatic vessel imaging[17,18] can mutually confirm the information both macroscopically and microscopically. We used FLAIR for colorectal imaging. An early study reported that FLAIR sequences are more sensitive to low gadolinium concentrations than T1-weighted sequences[19]. Another study showed that post-contrast FLAIR imaging may improve the lesion depiction when a higher lesion SI exists on the T2-weighted images[20]. A set of methods for quantitative MR imaging analysis were evaluated, and a standardized method was proposed[16]. We followed the suggested procedure in terms of ROI definition and SDNR calculation.

We reviewed the studies on intestinal particulate substance uptake, colon-specific drug delivery and DMH-induced intestinal and renal impairment in order to explain

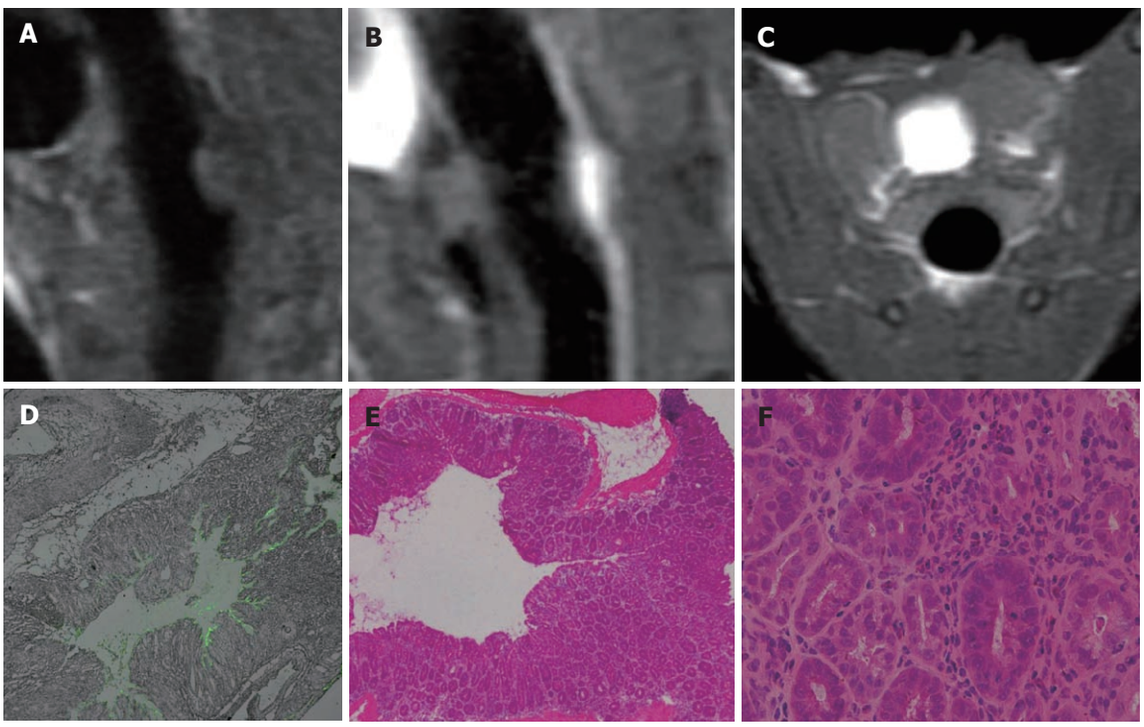

Figure 6 Peri-tumor interstitial fluorescein isothiocyanate deposition. A: A broad-based mass (high-level adenoma) in the pre-enema fluid attenuated inversion recovery (FLAIR) image; B, C: Tumor and peri-tumor mural enhancement, together with bladder imaging agent accumulation, in the post-enema FLAIR image; D: Interstitial linear fluorescein isothiocyanate deposition in the peri-tumor colorectal wall; E, F: Hematoxylin and eosin images at the same slice, obvious nuclear atypia identified.

the current results. It was proven, by lymph and plasma analysis, that more than 70% of the absorbed SLN was transported into systematic circulation *via* lymph, which is a major SLN transport pathway in the gastrointestinal tract[11]. Recent studies have further verified that the oral bioavailability of poorly water soluble contents (insulin, nitrendipine, tobramycin) increased significantly when encapsulated in the inner lipid matrix of SLNs[21,22].

The intestinal uptake of inert particles of the micrometer and nanometer range has been intensively studied in pharmaceutical research. The particles, usually used as oral drug delivery systems, include SLN (50-1000 nm), chitosan microspheres (2.1-12.5 μm), latex (2 μm), dendrimer and polymers, etc. The major conclusions of the studies[10,23-27] are summarized as follows. First, inert particulate uptake takes place along the entire length of the small and large intestines. Second, the process occurs not only *via* the M cells in the Peyer's patches and the isolated follicles of the gut-associated lymphoid tissue, but also *via* the normal intestinal enterocytes. Third, factors affecting the uptake include particle size, surface charge and surface modification. Larger (micrometer range) and surface modified particles may be retained for longer periods in the Peyer's patches, while smaller particles are transported to the thoracic duct. Fourth, an *in vitro* study using a Caco-2 cell model showed that 2 Gy X-irradiation increased particle (2 μm latex particles) uptake and translocation through the epithelium.

We hypothesize, based on the current results and earlier studies, that two different routes exist for the rectally administered SLN particles to enter the systematic circulation. In normal mice, the SLNs are mainly taken up by enterocytes and transferred to the lymphatic vessels and finally transported to the systematic circulation from the thoracic duct. In DMH-treated mice, however, the dominant route is from the carcinogen impaired colorectal mucosa, *via* the submucosal capillary network, to the mesenteric vein and then to the liver. As observed in this study, colorectal uptake and drainage of SLNs are an intracellular process; the transportation of SLNs in DMH-treated mice is a pathological process that occurs through an extracellular or interstitial route.

DMH and its metabolite azoxymethane (AOM) are specific colon carcinogens to model non-familial CRC in rodents[28]. Previous studies documented that DMH is also a renal carcinogen in mice[29-31]. The bladder gadolinium accumulation observed in this study may result from renal and intestinal epithelial impairment caused by DMH and its metabolites and the diuresis effect of manicol contained in SLN freeze-dried powder (20 mg /mL).

We believe that the bright rim sign in post-enema FLAIR images and corresponding cytoplastic FITC deposition in normal and group 1 mice is a manifestation of normal intestinal uptake function. Likewise, the halo sign observed in group 2 mice and linear extracellular FITC deposition is attributed to the impairment of intestinal epithelial barrier function. As functional changes always precede morphological lesions, further experiments are necessary to exemplify the early diagnostic potential by clarifying the mechanism at both cellular and

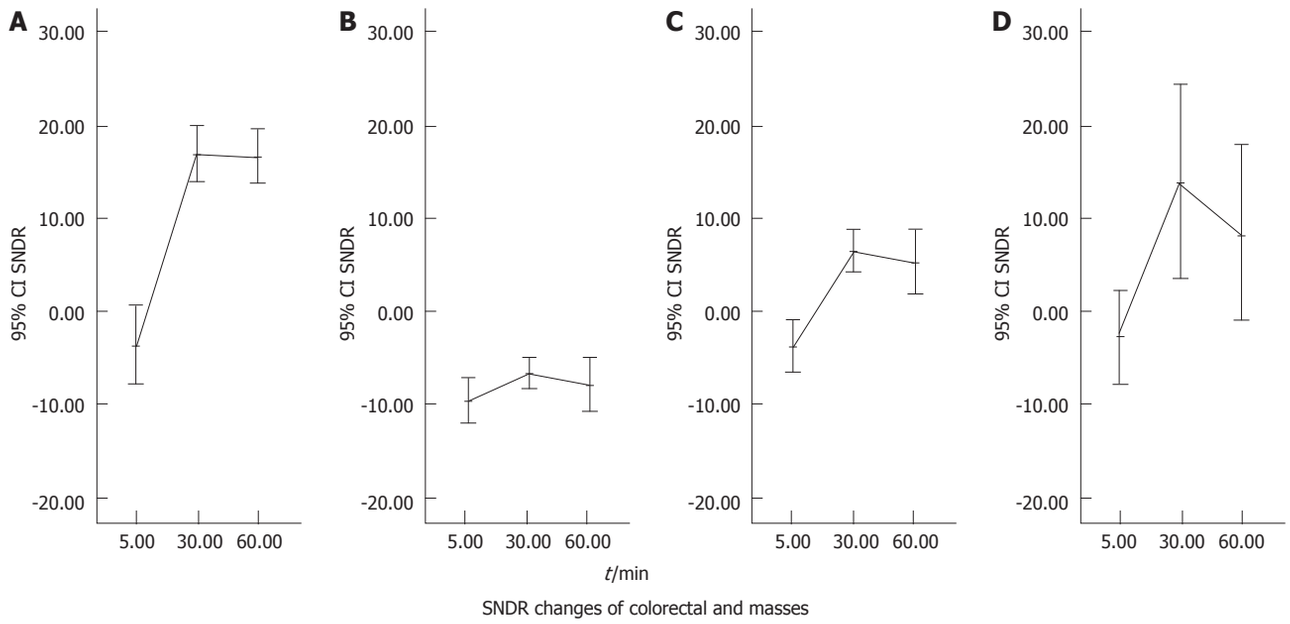

Figure 7 The signal intensity difference-to-noise ratios changes of colorectal wall and masses before and after the gadopentetate dimeglumine and fluorescein isothiocyanate-loaded solid lipid nanoparticle enema. A: The signal intensity difference-to-noise ratios (SDNRs) of colorectal wall in normal mice increased sharply after 20 min of the gadopentetate dimeglumine and fluorescein isothiocyanate-loaded solid lipid nanoparticle (Gd-FITC-SLN) enema ($P < 0.01$) and remain at a high level in the following 30 min with a minimum decrease ($P > 0.05$); B: The SDNRs of colorectal wall in group 1 [1,2-dimethylhydrazine (DMH) treated for 10 wk] increased significantly, with about one half of the amplitude compared with that of the normal mice, after the Gd-FITC-SLN enema; a visible decrease with no statistical significance ($P > 0.05$) of SDNRs occurred in the following 30 min; C: The SDNRs of colorectal wall in group 2 (DMH treated for 16 wk) increased and decreased non-significantly in post-enema images ($P > 0.01$); D: The SDNRs of intraluminal masses in DMH treated mice increased significantly ($P < 0.01$) and decreased non-significantly in the post-enema images ($P > 0.01$). SDNR: The Signal Intensity Difference–to-noise ratios.

molecular levels.

There were limitations in our study. First, layers of murine colorectal wall could not be differentiated on MR images due to the small animal size. We noticed that layers of the bowel and tumor invasion in the excised human colon cancer specimen were clearly depicted in one study[32]. Optimal delineation of layers of colorectal wall may likely be achieved if a porcine model was adopted. Second, sharp contrast in post-enema MR images (partial enhancement) existed but was rare, which may be explained by the diffuse impairment caused by DMH and its metabolite azoxymethane (AOM), delivered to the distal colorectum *via* the biliary system. Adoption of another colorectal tumor model, focally administered AOM, may improve the post-enema contrast between normal and cancerous tissues. Third, the long acquisition times of FLAIR pulse sequence may not be suitable for clinical MR colonography. More researches are, therefore, needed to optimize the technique in a clinical context.

COMMENTS

Background

High contrast between the bowel wall and lumen is essential for successful magnetic resonance (MR) colonography, which has been intensively studied in recent years. However, there has been no research aiming at MR visualizing the colorectal uptake of contrast medium.

Research frontiers

In this study, colorectal uptake of solid lipid nanoparticles (SLNs) in normal and dimethylhydrazine (DMH)-treated mice was visualized by MR and laser-scanning confocal fluorescence microscopic imaging.

Innovations and breakthroughs

Significant differences in colorectal uptake and distribution of SLNs were revealed in normal and DMH-treated mice, which may provide new mechanisms of contrast for MR colonography.

Applications

Direct and *in vivo* imaging of colorectal uptake of nanoparticles could be translated into radiological and pharmaceutical applications. Further work is needed to explore the potential value of current findings for personalized therapy and radiographic follow-up.

Terminology

SLNs are colloidal drug delivery systems with mean particle diameters ranging from 50 up to 1000 nm. SLNs combine the advantages of polymeric nanoparticles and fat emulsions for drug delivery administration, such as good tolerability, high oral bioavailability and large-scale production by high pressure homogenization. Magnetic resonance imaging is a cross-sectional imaging technique that does not utilize radiation and provides excellent tissue differentiation. MR colonography, based on the use of ultrafast MR sequences and relevant bowel contrast agents, is a less invasive colon imaging tool compared with optic colonoscopy.

Peer review

The authors concluded that the uptake of SLNs into the colon wall was significant difference between normal and 1, 2-DMH, specific colon carcinogens, treated mice. This paper has very interesting results, but the objective is not clear.

REFERENCES

1 **Geenen RW**, Hussain SM, Cademartiri F, Poley JW, Siersema PD, Krestin GP. CT and MR colonography: scanning techniques, postprocessing, and emphasis on polyp detection. *Radiographics* 2004; **24**: e18

2 **Ajaj W**, Lauenstein TC, Pelster G, Holtmann G, Ruehm SG, Debatin JF, Goehde SC. MR colonography in patients with incomplete conventional colonoscopy. *Radiology* 2005; **234**: 452-459

3 **Kuehle CA**, Langhorst J, Ladd SC, Zoepf T, Nuefer M, Gra-

bellus F, Barkhausen J, Gerken G, Lauenstein TC. Magnetic resonance colonography without bowel cleansing: a prospective cross sectional study in a screening population. *Gut* 2007; **56**: 1079-1085
4 **Zhang S**, Peng JW, Shi QY, Tang F, Zhong MG. Colorectal neoplasm: magnetic resonance colonography with fat enema-initial clinical experience. *World J Gastroenterol* 2007; **13**: 5371-5375
5 **Lauenstein TC**, Goehde SC, Ruehm SG, Holtmann G, Debatin JF. MR colonography with barium-based fecal tagging: initial clinical experience. *Radiology* 2002; **223**: 248-254
6 **Martin DR**, Yang M, Thomasson D, Acheson C. MR colonography: development of optimized method with ex vivo and in vivo systems. *Radiology* 2002; **225**: 597-602
7 **Lauenstein TC**, Schneemann H, Vogt FM, Herborn CU, Ruhm SG, Debatin JF. Optimization of oral contrast agents for MR imaging of the small bowel. *Radiology* 2003; **228**: 279-283
8 **Yeh P**, Ellens H, Smith PL. Physiological considerations in the design of particulate dosage forms for oral vaccine delivery. *Adv Drug Deliv Rev* 1998; **34**: 123-133
9 **Reis CP**, Ribeiro AJ, Houng S, Veiga F, Neufeld RJ. Nanoparticulate delivery system for insulin: design, characterization and in vitro/in vivo bioactivity. *Eur J Pharm Sci* 2007; **30**: 392-397
10 **Florence AT**. The oral absorption of micro- and nanoparticulates: neither exceptional nor unusual. *Pharm Res* 1997; **14**: 259-266
11 **Yuan H**, Chen J, Du YZ, Hu FQ, Zeng S, Zhao HL. Studies on oral absorption of stearic acid SLN by a novel fluorometric method. *Colloids Surf B Biointerfaces* 2007; **58**: 157-164
12 **Haupt S**, Rubinstein A. The colon as a possible target for orally administered peptide and protein drugs. *Crit Rev Ther Drug Carrier Syst* 2002; **19**: 499-551
13 **Reis CP**, Veiga FJ, Ribeiro AJ, Neufeld RJ, Damgé C. Nanoparticulate biopolymers deliver insulin orally eliciting pharmacological response. *J Pharm Sci* 2008; **97**: 5290-5305
14 **Uner M**, Yener G. Importance of solid lipid nanoparticles (SLN) in various administration routes and future perspectives. *Int J Nanomedicine* 2007; **2**: 289-300
15 **Yuan H**, Huang LF, Du YZ, Ying XY, You J, Hu FQ, Zeng S. Solid lipid nanoparticles prepared by solvent diffusion method in a nanoreactor system. *Colloids Surf B Biointerfaces* 2008; **61**: 132-137
16 **Pijl ME**, Doornbos J, Wasser MN, van Houwelingen HC, Tollenaar RA, Bloem JL. Quantitative analysis of focal masses at MR imaging: a plea for standardization. *Radiology* 2004; **231**: 737-744
17 **Cai W**, Chen X. Multimodality molecular imaging of tumor angiogenesis. *J Nucl Med* 2008; **49 Suppl 2**: 113S-128S
18 **Mounzer R**, Shkarin P, Papademetris X, Constable T, Ruddle NH, Fahmy TM. Dynamic imaging of lymphatic vessels and lymph nodes using a bimodal nanoparticulate contrast agent. *Lymphat Res Biol* 2007; **5**: 151-158
19 **Ercan N**, Gultekin S, Celik H, Tali TE, Oner YA, Erbas G. Diagnostic value of contrast-enhanced fluid-attenuated inversion recovery MR imaging of intracranial metastases. *AJNR Am J Neuroradiol* 2004; **25**: 761-765
20 **Kubota T**, Yamada K, Kizu O, Hirota T, Ito H, Ishihara K, Nishimura T. Relationship between contrast enhancement on fluid-attenuated inversion recovery MR sequences and signal intensity on T2-weighted MR images: visual evaluation of brain tumors. *J Magn Reson Imaging* 2005; **21**: 694-700
21 **Kumar VV**, Chandrasekar D, Ramakrishna S, Kishan V, Rao YM, Diwan PV. Development and evaluation of nitrendipine loaded solid lipid nanoparticles: influence of wax and glyceride lipids on plasma pharmacokinetics. *Int J Pharm* 2007; **335**: 167-175
22 **Manjunath K**, Venkateswarlu V. Pharmacokinetics, tissue distribution and bioavailability of nitrendipine solid lipid nanoparticles after intravenous and intraduodenal administration. *J Drug Target* 2006; **14**: 632-645
23 **Smyth SH**, Feldhaus S, Schumacher U, Carr KE. Uptake of inert microparticles in normal and immune deficient mice. *Int J Pharm* 2008; **346**: 109-118
24 **Moyes SM**, Killick EM, Morris JF, Kadhim MA, Hill MA, Carr KE. Changes produced by external radiation in parameters influencing intestinal permeability and microparticle uptake in vitro. *Int J Radiat Biol* 2008; **84**: 467-486
25 **Doyle-McCullough M**, Smyth SH, Moyes SM, Carr KE. Factors influencing intestinal microparticle uptake in vivo. *Int J Pharm* 2007; **335**: 79-89
26 **Smyth SH**, Doyle-McCullough M, Cox OT, Carr KE. Effect of reproductive status on uptake of latex microparticles in rat small intestine. *Life Sci* 2005; **77**: 3287-3305
27 **Hussain N**, Jaitley V, Florence AT. Recent advances in the understanding of uptake of microparticulates across the gastrointestinal lymphatics. *Adv Drug Deliv Rev* 2001; **50**: 107-142
28 **Bissahoyo A**, Pearsall RS, Hanlon K, Amann V, Hicks D, Godfrey VL, Threadgill DW. Azoxymethane is a genetic background-dependent colorectal tumor initiator and promoter in mice: effects of dose, route, and diet. *Toxicol Sci* 2005; **88**: 340-345
29 **Turusov VS**, Lanko NS, Parfenov IuD, Chemeris GIu. [1,2-dimethylhydrazine induction of epithelial tumors of the kidneys in CBA strain mice]. *Eksp Onkol* 1990; **12**: 71-74
30 **Chemeris GIu**, Poltoranina VS, Turusov VS. [Histogenesis of experimental renal tumors in mice]. *Arkh Patol* 1992; **54**: 48-52
31 **Turusov VS**. Renal cell tumors induced in CBA male mice by 1,2-dimethylhydrazine. *Toxicol Pathol* 1992; **20**: 570-575
32 **Yamada I**, Okabe S, Enomoto M, Sugihara K, Yoshino N, Tetsumura A, Kumagai J, Shibuya H. Colorectal carcinoma: in vitro evaluation with high-spatial-resolution 3D constructive interference in steady-state MR imaging. *Radiology* 2008; **246**: 444-453

S- Editor Tian L **L- Editor** Ma JY **E- Editor** Xiong L